Amino Acid Differences at Positions 10, 11, and 104 Explain the Profound Catalytic Differences between Two Murine Pi-Class Glutathione *S*-Transferases

Theo K. Bammler,[‡] Huub Driessen,[§] Niklas Finnstrom,[‡,||] and C. Roland Wolf*[,‡]

Imperial Cancer Research Fund, Molecular Pharmacology Unit, Biomedical Research Centre, Ninewells Hospital and Medical School, Dundee DD1 9SY, Scotland, and Imperial Cancer Research Fund, Unit of Structural Molecular Biology, Department of Crystallography, Birkbeck College, Malet Street, London WC1E 7HX, England

Received February 2, 1995; Revised Manuscript Received April 14, 1995[⊗]

ABSTRACT: The glutathione *S*-transferases play a pivotal role in the detoxification of toxic and carcinogenic electrophiles. We have previously reported the isolation of two actively transcribed murine pi-class glutathione *S*-transferase genes. In this study the two proteins encoded by these genes, Gst p-1 and Gst p-2, were expressed in *Escherichia coli* and found to exhibit profoundly different catalytic activities, the activity of Gst p-2 toward a panel of electrophilic substrates being 1−3 orders of magnitude lower than that of Gst p-1. In order to establish the basis for the difference between these highly homologous proteins, mutants were generated where specific amino acids had been exchanged. Kinetic analysis of the wild-type and mutant enzymes revealed that the amino acid differences occurring at positions 10 (Val/Ser), 11 (Arg/Pro), and 104 (Val/Gly) are responsible for the reduced enzymatic activity of Gst p-2. This analysis together with computer graphics modeling for Gst p-2 indicated that these changes affected both substrate and glutathione binding to the enzyme.

Cytosolic glutathione *S*-transferases (GSTs)[1] are a family of dimeric enzymes which play a pivotal role in the conjugation of reduced glutathione (GSH) to a wide range of lipophilic electrophiles, including carcinogens and other toxins (Coles & Ketterer, 1990). Furthermore, certain GSTs catalyze the reduction of organic peroxides and protect membranes and DNA from oxidative damage (Ketterer et al., 1987). These enzymes also play a role in the intracellular transport and storage of hydrophobic molecules like hematin, bilirubin, and bile salts (Listowsky et al., 1988). In addition to their role as detoxification enzymes, GSTs also catalyze the isomerization of 3-ketosteroids and are involved in the biosynthesis of leukotrienes (Benson et al., 1977).

On the basis of nucleotide and amino acid sequence similarities, mammalian cytosolic GSTs can be grouped into four classes termed alpha, mu, pi, and theta (Mannervik et al., 1985, 1992; Meyer et al., 1991). Members within a class can form homo- or heterodimers which possess one active site per subunit. Recent reports on the crystal structures of alpha, mu, and pi class GSTs have had a tremendous impact on our understanding of the molecular architecture and function of these enzymes (Reinemer et al., 1991, 1992; Ji et al., 1992; Sinning et al., 1993; Garcia-Saez et al., 1994). Following the observation of Sato and co-workers that the pi-class GST is markedly elevated in rat liver tumor development (Sato et al., 1984a,b), much attention has focused on this group of enzymes. Subsequent studies demonstrated that this protein is one of the most reliable markers for pre-neoplastic lesions during rat liver carcinogenesis (Sato, 1989). Furthermore, several reports showed a significant increase in the levels of pi-class GST in a number of human tumors including oral, colon, stomach, and lung (Sato, 1989; Howie et al., 1990; Black & Wolf, 1991; Volm et al., 1991). In addition, these enzymes are expressed at elevated levels in cell lines made resistant to anticancer drugs and chemical toxins (Batist et al., 1986; Cowan et al., 1986; Wolf et al., 1990; Black & Wolf, 1991).

Inspite of numerous studies, the precise role of pi-class GSTs in carcinogenesis and multidrug resistance remains unclear. In order to answer these questions, we have been studying pi-class genes in the mouse because of the ability to apply mouse genetics to this problem, particularly because of the ability to generate transgenic animals and to carry out gene targeting experiments.

Recently, we reported the cloning of two actively transcribed murine pi-class GST genes, as well as their cDNAs (Bammler et al., 1994). In the present study, we have characterized the proteins encoded by these genes in detail and related amino acid differences to the observed profound differences in catalytic activity.

EXPERIMENTAL PROCEDURES

Materials. All chemicals were of analytical grade or better and were purchased from either Sigma Chemical Co., Poole, Dorset, U.K., or BDH, Glasgow, U.K., unless otherwise indicated. Restriction endonucleases used in this study were obtained from Gibco BRL (Life Technologies Ltd., Paisley, Renfrewshire, Scotland, U.K.).

Generation of Mutant GST cDNAs. The two GST cDNAs, Gst p-1 and Gst p-2, were isolated as described previously (Bammler et al., 1994). The oligonucleotides used for site-directed mutagenesis of Gst p-1 are listed in Table 1. The Gst p-1 cDNA was cloned into the *Eco*RI and *Xba*I restriction sites of the pAlter vector (Promega, Madison, WI),

* Author for correspondence.
‡ Ninewells Hospital and Medical School.
§ Birkbeck College.
|| Current address: Department of Clinical Pharmacology, University Hospital, S-751 85 Uppsala, Sweden.
⊗ Abstract published in *Advance ACS Abstracts,* June 15, 1995.
[1] Abbreviations: CDNB, 1-chloro-2,4-dinitrobenzene; DCNB, 2,4-dichloro-4-nitrobenzene; GST, glutathione *S*-transferase; GSH, glutathione.

0006-2960/95/0434-9000$09.00/0

Table 1: Oligonucleotide Primers Used for Site-Directed Mutagenesis

mutant	amino acid changed in Gst p-1	oligonucleotide sequence[a]	sense
P1-V10S	Val10 → Ser	5′-TCACACCGCCCTCGACTTGGGAAGTAGACAAT-3′	inverse
P1-R11P	Arg11 → Pro	5′-CACACCGCCCTGGAACTGGGAAG-3′	inverse
P1-M89V	Met89 → Val	5′-CACCATATCCACCTGGGCGGCCT- 3′	inverse
P1-V104G	Val104 → Gly	5′-GATGAGGGTGCCATATTTGCCGC-3′	inverse
P1-L106M	Leu106 → Met	5′-ATAGTTGGTGTAGATCATGGTGACATATTTGCC-3′	inverse
P1-T109R	Thr109 → Arg	5′-ATTCTCATAGTTTCTGTAGATGAGGG-3′	inverse

[a] Mismatches between the mutagenic oligonucleotide and the cDNA of GST p-1 are underlined.

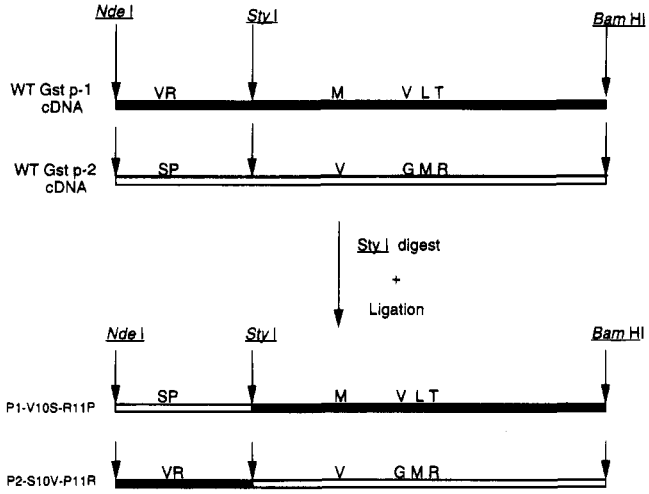

FIGURE 1: Schematic diagram showing the generation of the double mutant cDNAs P1-V10S-R11P and P2-S10V-P11R. The *Nde*I/*Sty*I fragment of the wild-type (WT) cDNA Gst p-1 was ligated with the *Sty*I/*Bam*HI fragment of the wild-type cDNA Gst p-2 and *vice versa*. The six amino acid differences between the two wild-type cDNAs are indicated by single-letter abbreviations.

and oligonucleotide-directed mutagenesis was carried out according to the manufacturer's recommendations. An overall success rate of 73% was achieved using the pAlter mutagenesis system.

Both murine pi-class cDNAs, Gst p-1 and Gst p-2, contain a unique *Sty*I restriction site 215 base pairs downstream of the ATG start codon. This enabled us to generate chimeric cDNAs, which contain the 5′ end of Gst p-1 and the 3′ end of Gst p-2, and *vice versa* (Figure 1). Briefly, the *Sty*I fragments of the two cDNAs were gel purified, and the appropriate fragments were ligated using T4 DNA ligase (Boehringer, Mannheim, Germany). The entire sequence of all mutant cDNAs was determined by the chain termination method of Sanger et al. (1977) before they were used for heterologous expression in *Escherichia coli*.

Expression and Purification of Murine Pi-Class GSTs. The pET expression system (AMS Biotechnology U.K. Ltd., Witney, Oxon, England) was used to express the wild-type and mutant GSTs. Expression was carried out according to the manufacturer's instructions. Briefly, all cDNAs were cloned into the *Nde*I and *Bam*HI restriction sites of the expression vector pET-21a, and the GSTs were transfected into the *E. coli* strain BL21(DE3). Expression was induced with a 2-h exposure to 1 mM isopropylthiogalactose (Boehringer), after which time the bacteria were harvested by centrifugation at 10000*g* for 15 min. Harvesting and all of the following steps were carried out at 4 °C. The cell pellet was resuspended in buffer A (50 mM Tris-HCl, pH 7.4, 200 mM NaCl, 0.5 mM dithiothreitol), and the bacterial cells were lysed by ultrasonication. Intact cells and cell debris were removed by two centrifugation steps at 50000*g* for 30 min each time. The resulting supernatant was loaded onto a glutathione−agarose affinity column, which had been equilibrated previously with buffer A. The bound protein was washed with approximately 15 column volumes of buffer A, and the recombinant GSTs were eluted with buffer B (200 mM Tris-HCl, pH 9.0, 50 mM glutathione). The absorbance at 280 nm of the collected fractions (1.5 mL each) was measured. Fractions showing an absorbance value >0.8 were pooled and dialyzed against four changes of 2 L of buffer C (40 mM sodium phosphate buffer, pH 7.4, 0.5 mM dithiothreitol, 0.5 mM EDTA). The purified proteins were frozen on dry ice and stored at −70 °C for up to 8 weeks, without a significant loss of activity. The purity of the proteins was analyzed by SDS/PAGE (Laemmli, 1970). When the same procedure was repeated using *E. coli* BL21-(DE3), which did not harbor the expression vector, no bacterial protein bound to the affinity column.

Enzyme Assays. All enzyme assays were carried out at 30 °C. The 1-chloro-2,4-dinitrobenzene (CDNB) assay was carried out using a Cobas Fara centrifugal analyzer as described by Hayes and Clarkson (1982). Assays with either 1,2-dichloro-4-nitrobenzene (DCNB, Aldrich Chemical Co. Ltd., Gillingham, Dorset, England, U.K.), ethacrynic acid, bromosulfophthalein, *trans*-4-phenyl-3-buten-2-one (Aldrich), 1,2-epoxy-3-(*p*-nitrophenoxy)propane, *p*-nitrobenzyl chloride, *p*-nitrophenyl acetate, or Δ^5-androstene-3,17-dione were performed as described by Habig et al. (1974, 1981). Selenium-independent glutathione peroxidase activity for organic hydroperoxide was determined by using the coupled assay system described by Reddy et al. (1981). Protein concentrations were determined by the method of Lowry et al. (1951) using bovine serum albumin as a standard.

Kinetic Analysis. Activity toward CDNB was assayed spectrophotometrically at 340 nm using a Cobas Fara centrifugal analyzer. Assays were performed in triplicate at 30 °C. Initial rates were measured at 5 s intervals for a total period of 55 s, commencing 3 s after initial mixing. The reaction was initiated by the addition of the enzyme to 0.1 M sodium phosphate buffer, pH 6.5, containing the substrates CDNB and GSH. CDNB was dissolved in ethanol, and the final concentration of ethanol in the reaction mixture was constant at 3.5%. Nonenzymatic reaction rates were subtracted from enzymatic rates. The enzymatic rate was linear with time for up to 60 s after initiation. Each data point represents the mean of three measurements. Individual kinetic parameters represent the mean of three independent series of experiments, with the only exception being the values for Gst p-2 which are calculated from two experiments. Kinetic analysis was based on the report by Phillips and Mantle (1991) describing the initial rate kinetics of murine pi-class GST YfYf (Gst p-1) as a rapid-equilibrium random mechanism. Therefore, initial velocities can be

interpreted according to the equation:

$$V_0 = \frac{V_{max}AB}{\alpha K_A K_B + \alpha K_B A + \alpha K_A B + AB}$$

(A, GSH; B, CDNB). Double-reciprocal plots of initial velocitiy data were linear for all enzymes. Individual kinetic parameters were determined as described by Ivanetich and Gould (1989). Regression analysis was performed using the Apple Mac program Cricket Graph, version 1.3.2. With CDNB as the varied substrate, GSH concentrations ranged from 0.05 to 2 mM. With GSH as the varied substrate, CDNB concentrations ranged from 0.1 to 2 mM (the CDNB concentration cannot be increased above 2 mM for reasons of solubility).

Model Building. The sequence of mouse Gst p-2 was modeled into the 1.8 Å three-dimensional structure of Gst p-1 (Garcia-Saez et al., 1994) by computer graphics on an Evans and Sutherland PS390, using the FRODO program (Jones, 1978, as modified by P. Evans). Side chains which were not identical were placed in similar positions and then adjusted interactively to minimize unfavorable contacts and to optimize van der Waals and electrostatic interactions, keeping in mind the need to form a close-packed core. Where necessary, other residues were adjusted. The resulting coordinates were also compared with those of pig lung P-1 GST (Reinemer et al., 1991). Water accessibilities were calculated using the program DSSP of Kabsch and Sander (1983). Contacts were calculated with the program MODEL (Driessen, unpublished). Residues for Gst p-2 are numbered according to the mouse liver Gst p-1 structure.

RESULTS

Catalytic Activities of Two Recombinant Wild-Type Murine Pi-Class GSTs. We recently reported the cloning of a novel murine pi-class glutathione *S*-transferase cDNA termed Gst p-2 (Bammler et al., 1994). N-Terminal sequence comparison showed that Gst p-2 is different from the murine pi-class GST reported by Mannervik and colleagues (1985) and Hatayama et al. (1990). In order to obtain Gst p-1 (YfYf, MII) and Gst p-2 protein, their corresponding cDNAs were expressed in *E. coli*. Immunoblotting of the soluble fractions of individual *E. coli* cultures showed that both constructs expressed GST protein at very similar levels (results not shown). The recombinant enzymes were purified on a glutathione−agarose affinity column to apparent homogeneity as judged by SDS/PAGE analysis (Figure 2). One litre of *E. coli* culture yielded approximately 60 mg of pure Gst p-1 protein, whereas only approximately 15 mg of Gst p-2 was obtained. This suggested that Gst p-2 bound with a lower affinity to the glutathione−agarose column. The relative mobilities of the proteins in SDS/PAGE were indistinguishable, with an apparent molecular mass of 23.5 kDa (Figure 2). In order to establish whether the two enzymes have similar or distinct catalytic activities, we determined their activity toward a panel of established GST substrates (CDNB, DCNB, bromosulfophthalein, ethacrynic acid, *trans*-4-phenyl-3-butene-2 one, 1,2-epoxy-3-(*p*-nitrophenoxy)propane, cumene hydroperoxide, *p*-nitrophenyl acetate, *p*-nitrobenzyl chloride, Δ^5-androstene-3,17-dione) (Table 2). Gst p-1 was much more active toward all of these substrates than Gst p-2.

FIGURE 2: Purified recombinant wild-type and mutant murine pi-class glutathione *S*-transferase proteins. Purified recombinant wild-type (WT) and mutant murine pi-class GSTs were analyzed by SDS/PAGE in 12% polyacrylamide resolving gels. The gel was loaded as follows: STD, molecular weight standards; lanes 1 and 12, mouse Yf marker isolated from mouse liver; lane 2, WT Gst p-1; lane 3, WT Gst p-2; lane 4, P1-V10S-R11P; lane 5, P2-S10V-P11R; lane 6, P1-V10S; lane 7, P1-R11P; lane 8, P1-M89V; lane 9, P1-V104G; lane 10, P1-L106M; lane 11, P1-T109R. Panel A shows the polyacrylamide gel stained with Coomassie Blue R250 (1 μg of protein was loaded per lane); panel B shows the immunoblot developed with a polyclonal antibody raised against purified pi-class GST (YfYf) isolated from mouse liver (100 ng of protein was loaded per lane).

Table 2: Specific Activities (μmol min^{-1} mg^{-1}) of the Two Wild-Type Murine Pi-Class GSTs, Gst p-1 and Gst p-2[a]

substrate	Gst p-1	Gst p-2
1-chloro-2,4-dinitrobenzene	84 ± 4	0.12 ± 0.01
1,2-dichloro-4-nitrobenzene	0.10 ± 0.01	ND
bromosulfophthalein	ND	ND
ethacrynic acid	6.1 ± 0.5	0.04 ± 0.008
trans-4-phenyl-3-buten-2-one	0.016 ± 0.0008	ND
1,2-epoxy-3-(*p*-nitrophenoxy)propane	0.45 ± 0.017	ND
cumene hydroperoxide	0.09 ± 0.01	0.01 ± 0.001
p-nitrophenyl acetate	0.21 ± 0.012	ND
p-nitrobenzyl chloride	1.24 ± 0.085	0.05 ± 0.01
Δ^5-androstene-3,17-dione	0.09 ± 0.004	ND

[a] All analyses were performed at least in triplicate (±SD); ND, not detectable.

Expression of Mutant Murine Pi-Class GSTs. There are six amino acid differences between Gst p-1 and Gst p-2 in two clusters: one located in the N-terminal domain (amino acids 10 and 11) and the other in the C-terminal domain (amino acids 89, 104, 106, and 109). In order to assess the contribution of each of the six amino acid differences between Gst p-1 and Gst p-2 to the profound difference in enzymatic activity, six mutants of Gst p-1 were created, where one single amino acid was replaced with the equivalent amino acid in Gst p-2 (Table 1). In addition, two hybrid enzymes were generated, in which the N-termini, containing the amino acid differences Val/Ser10 and Arg/Pro11, were interchanged. These hybrid enzymes were designed to examine the possible combined effect of the amino acid differences. To characterize the mutant enzymes further, they were expressed and purified (Figure 2). All mutant proteins were expressed at very similar levels as judged by immunochemical analysis of the soluble fractions of individual *E. coli* cultures (results not shown). They all bound to the GSH affinity column, and approximately 60 mg of pure protein was obtained from a 1 L culture, with the exception of the mutants P1-R11P and P1-V10S-R11P.

Table 3: Kinetic Constants for Wild-Type and Mutant Enzymes in the Reaction Involving CDNB as the Electrophilic Substrate[a]

			GSH		CDNB	
enzyme	V_{max} (μmol min^{-1} mg^{-1})	k_{cat} (s^{-1})	K_m^{GSH} (mM)	k_{cat}/K_m^{GSH} (mM^{-1} s^{-1})	K_m^{CDNB} (mM)	k_{cat}/K_m^{CDNB} (mM^{-1} s^{-1})
wild type						
Gst p-1	141.1 ± 6.3	55.5 ± 2.5	0.12 ± 0.01	446 ± 33	0.75 ± 0.11	75 ± 6
Gst p-2	0.8[b]	0.3[b]				
double mutants						
P1-V10S-R11P	1.7 ± 0.4	0.7 ± 0.2	3.27 ± 0.52	0.2 ± 0.007	2.22 ± 0.58	0.3 ± 0.04
P2- S10V-P11R	73.9 ± 9.5	29.2 ± 3.7	0.38 ± 0.09	81 ± 10	2.84 ± 0.25	10 ± 0.8
single mutants						
P1-V10S	28.2 ± 4.0	11.1 ± 1.6	0.07 ± 0.02	163 ± 10	0.43 ± 0.09	24 ± 3
P1-R11P	4.7 ± 1.6	1.8 ± 0.6	2.86 ± 0.23	0.46 ± 0.04	1.52 ± 0.42	1.6 ± 0.3
P1-M89V	172.6 ± 8.5	67.8 ± 3.4	0.21 ± 0.05	371 ± 63	0.55 ± 0.18	134 ± 23
P1-V104G	62.9 ± 3.8	24.7 ± 1.5	0.28 ± 0.08	100 ± 18	2.24 ± 0.29	11 ± 0.6
P1-L106M	120.6 ± 7.7	47.5 ± 3.0	0.15 ± 0.03	321 ± 29	0.60 ± 0.03	79 ± 0.4
P1-T109R	116.7 ± 8.4	46.0 ± 3.3	0.14 ± 0.05	293 ± 23	0.70 ± 0.06	65 ± 1

[a] Values represent the means (±SD) of three independent series of measurements as described in Experimental Procedures. [b] Mean calculated from two series of measurements only; therefore, no standard deviation is provided.

These two mutants bound with lower affinity to the glutathione−agarose column, resulting in an approximately 4-fold lower yield of purified proteins. All mutant proteins displayed the same mobility and were stable as judged by SDS/PAGE analysis.

Kinetic Analysis of the Wild-Type and Mutant Enzymes. The kinetic properties of the purified wild-type and mutant enzymes in the conjugation of CDNB with GSH are shown in Table 3. Due to the very low activity, the wild-type enzyme Gst p-2 could not be reliably characterized. Kinetic analysis revealed that the wild-type enzyme Gst p-1 and the mutants P1-M89V, P1-L106M, and P1-T109R exhibited similar kinetic properties. In contrast, the mutants P1-V10S, P1-R11P, and P1-V104G displayed significantly lower catalytic efficiencies (k_{cat}/K_m) than Gst p-1. The k_{cat} values for P1-V10S, P1-R11P, and P1-V104G were 80%, 97%, and 55% decreased, respectively, as compared to the wild-type Gst p-1. There was an approximately 2-fold increase in the K_m value for CDNB for the mutant P1-R11P, whereas the mutant P1-V104G showed a 3-fold higher value. While an approximately 2-fold change in K_m for GSH was observed for P1-V104G, a profound increase of approximately 24-fold was measured for P1-R11P. Interestingly, the P1-V10S mutant did not exhibit a significant change in K_m for either CDNB or GSH. The hybrid enzyme P1-V10S-R11P gave kinetic constants very similar to those observed for the single mutant, P1-R11P. The wild-type enzyme Gst p-2 had a k_{cat} value of approximately 0.5% of Gst p-1. When both Ser10 and Pro11 were replaced by Val and Arg (P2-S10V-P11R) in Gst p-2, the k_{cat} value of Gst p-2 increased approximately 97-fold and reached approximately 53% of the value of Gst p-1.

Kinetic constants for the two single mutants P1-V10S and P1-R11P and the hybrid enzymes P1-V10S-R11P and P2-S10V-P11R strongly suggest that the two amino acid differences between Gst p-1 and Gst p-2 at positions 10 and 11 are major determinants for the catalytic activity differences of the two wild-type enzymes. In addition, the replacement of Val104 by Gly has also a significant effect on the wild-type enzyme Gst p-1, lowering the k_{cat} value approximately 55% and increasing the K_m for GSH and CDNB approximately 2- and 3-fold, respectively.

Relationship between the Activity of the Mutants and the Three-Dimensional Model of Mouse Gst p-2. In order to rationalize the different activities of the mutant proteins, a model for Gst p-2 was constructed on the basis of the three-dimensional coordinates of the crystal structure of Gst p-1, complexed with *S*-(*p*-nitrobenzyl)glutathione (Garcia-Saez et al., 1994). Alignment of Gst p-1 and Gst p-2 was unambiguous as the sequences have an equal number of amino acids with only six differences in 209 residues (Figure 3). These data are discussed below.

DISCUSSION

Unlike other species characterized to date, the mouse contains two actively transcribed pi-class GST genes. The recombinant proteins encoded by these genes exhibit a profound difference in enzymatic activity. The catalytic activity of Gst p-1 was extremely similar to the GST pi form isolated previously from mouse liver (Warholm et al., 1986; McLellan et al., 1987). Importantly, the kinetic parameters for Gst p-1 were very similar to those reported for the murine pi-class GST isolated by Phillips and Mantle (1991). In contrast, the specific activities of Gst p-2 for the substrates CDNB, ethacrynic acid, *p*-nitrobenzyl chloride, and cumene hydroperoxide were 700-, 150-, 25-, and 9-fold lower, respectively. Furthermore, Gst p-2 was not catalytically active toward any of the other substrates tested. This marked difference in catalytic activity could be considered surprising, as the two proteins share 97% sequence identity. As the two enzymes differ in only six amino acids, it was possible to examine which of these are responsible for the differences observed in catalytic activity of Gst p-2.

Recently, crystal structures of mammalian GSTs, belonging to the alpha, mu, and pi class, have been solved, and the molecular architecture of the active site has been determined. Each subunit of the dimeric enzyme has an active site which is composed of two distinct functional regions: a hydrophilic G-site which binds the physiological substrate GSH and an adjacent H-site which provides a hydrophobic environment for the binding of structurally diverse electrophilic substrates (Mannervik et al., 1988; Reinemer et al., 1991, 1992). The outer wall of the active site cave is made up by helix αB and helix 3_{10}B connecting it to strand β3, the inner wall by the C-terminal part of helix αD, the C-terminus, and the middle of helix αD of the neighboring subunit, and the bottom by the segment between strand β1 and αA. The differences between Gst p-1 and Gst p-2 are concentrated in just two secondary structure elements located at the bottom and the inner wall of the active site (Figure 4a). Residues

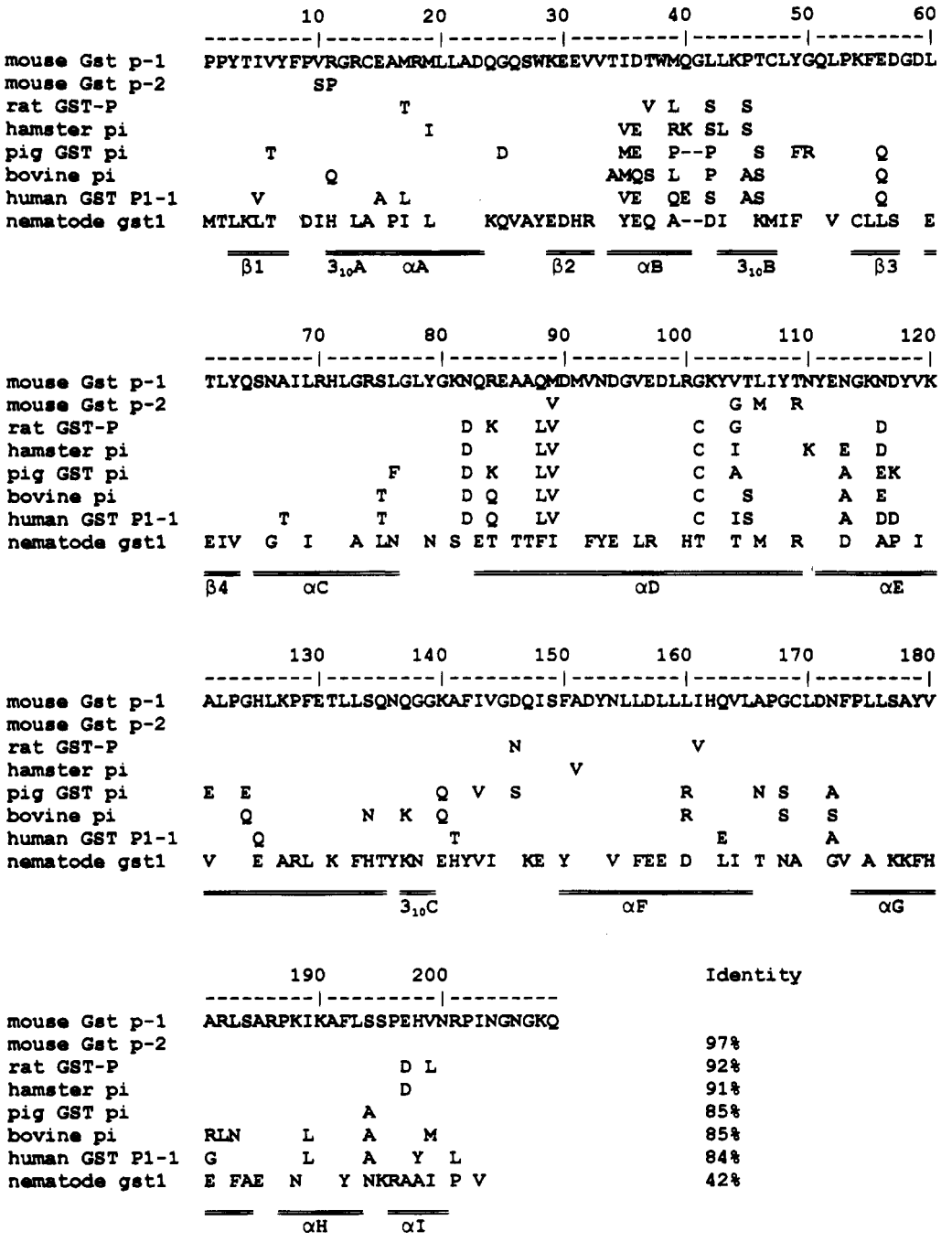

FIGURE 3: Sequence alignment of all known GST pi sequences. Sequence identities are given with respect to mouse Gst p-1. The secondary structure elements as determined for this protein (Garcia-Saez et al., 1994) are indicated with a double line. Sequences are from Bammler et al. (1994), Suguoka et al. (1985), Swedmark and Jensson (1994), Dirr et al. (1991), Hernando et al. (1991), Kano et al. (1987), and Weston et al. (1989).

10 and 11 are positioned on the segment between strand $\beta 1$ and αA comprising a γ-turn followed by a 3_{10} helix, while residues 89, 104, 106, and 109 are situated on helix αD, the latter three in the C-terminal part.

The residues in the H-site of Gst p-1 are all hydrophobic and are highly conserved: Phe8, Val10, Ile35, Tyr108, the Cα of Gly205, while Pro9 and Pro202 are in the vicinity (Reinemer et al., 1991; Garcia-Saez et al., 1994). In monomer A of the structure of murine Gst p-1, the hydroxyl group of Tyr108 points toward the plane of the aromatic ring of the *S-p*-nitrobenzyl group and is within van der Waals contact range of the Cε, Cζ2, and Cγ2 atoms, in subunit B also of Cζ1 (Figure 4b). Val10 interacts with the edge of the aromatic ring of the *S-p*-nitrobenzyl group.

When Val10 was replaced by Ser in Gst p-1, the catalytic efficiency ($k_{cat}/K_m^{GSH/CDNB}$) decreased approximately 3-fold. This was due to an approximately 5-fold decreased k_{cat} value and somewhat lower K_m values for both CDNB and GSH. The binding of GSH therefore does not appear to be affected significantly. As described above, Val10 participates directly in the lining of the H-site and is within van der Waals range of the ring of Tyr7. Moreover, this residue is conserved in all mammalian pi-class GSTs isolated so far, the only exception being Gst p-2 (Figure 3). In addition, in the pi-class GST isolated from the nematode *Caenorhabditis elegans* (Weston et al., 1989) Val10 is replaced conservatively by Ile (Figure 3). In the mu-class GST the comparable residue is implicated in control of stereoselectivity (Ji et al.,

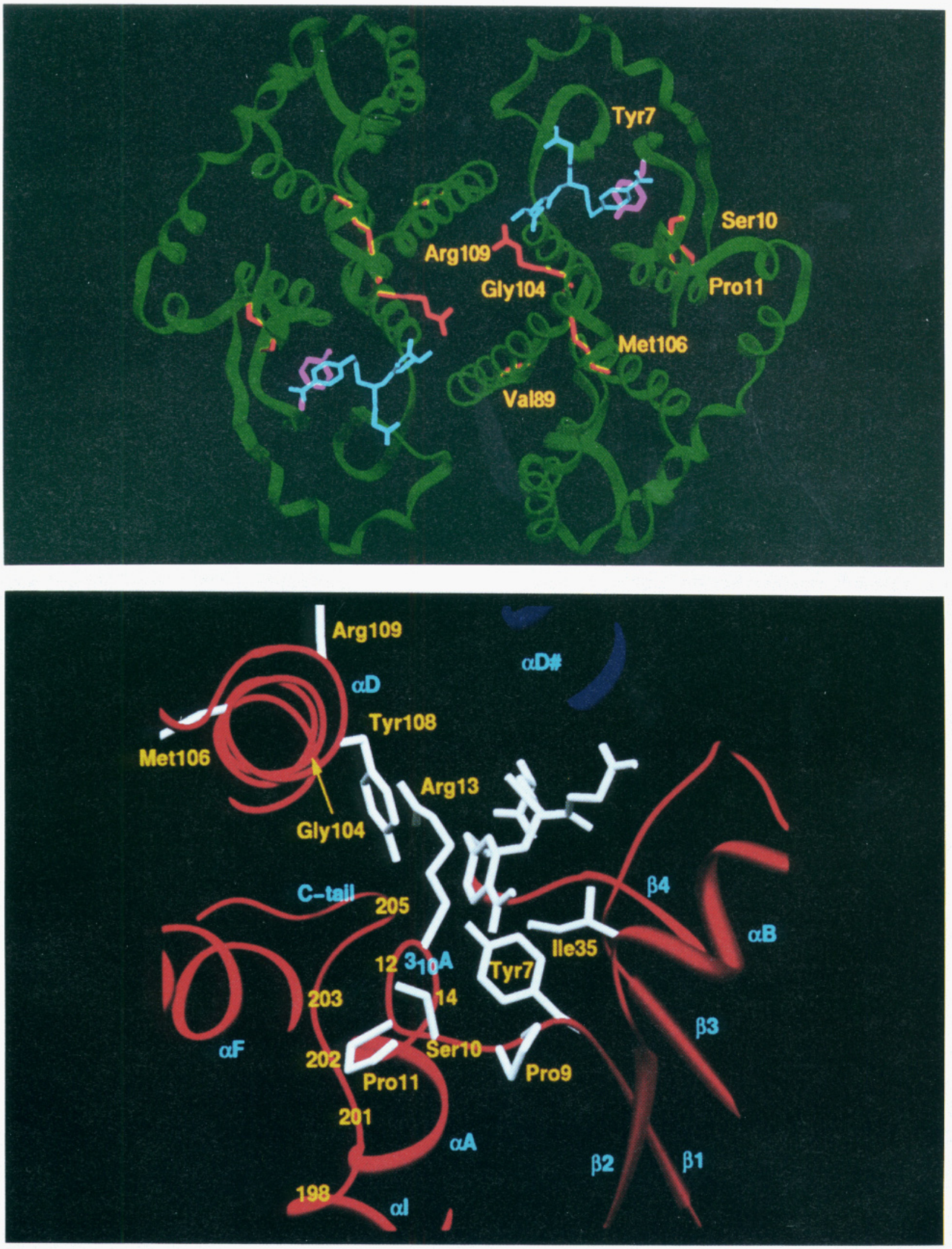

FIGURE 4: Predicted structures of Gst p-2. (a, top) Ribbon diagram of the mouse Gst p-2 model, based on the structure of mouse Gst p-1. The GSH−substrate conjugate is shown in blue, Tyr7 is in purple, and the side chains of the six amino acids which differ between Gst p-1 and p-2 are in red. (b, bottom) Active site of the Gst p-2 model, based on the structure of mouse Gst p-1. The secondary structure elements are shown as red and blue ribbons and are identified in pale blue. The GSH−substrate conjugate and the side chains of relevant residues are shown in white and are identified in yellow. Where necessary, the positions of other residues are indicated by a yellow number only.

1994). These observations therefore rationalize the reduction in enzyme activity when the hydrophobic residue Val10 is replaced by the more hydrophilic Ser residue. On the basis of the above arguments it would be expected that the affinity of the mutant P1-V10S for CDNB would be decreased significantly as compared to Gst p-1. However, judging by the K_m, this was not the case.

If the hydroxyl group of Ser 10 points toward the substrate, which would require some main-chain movement, Tyr108 and Ser10 could both be involved in electrophilic assistance in addition to GSH to an as yet unknown substrate in a similar way as has been shown for the equivalent Tyr115 in mu3-3 (Ji et al., 1994). Tyr108 is about 2.8 Å deeper in the active site of Gst p-1 than in the mu class, while no equivalent to mu Ser209 is hydrogen-bonded. In the model, the OH of Tyr108 and the Cβ of Ser10 are 5.85 Å apart (Figure 4b). In this respect it is noteworthy that theta-class GSTs do possibly have a Ser in this area, while dog theta (YdfYdf) has the combination Ser-Pro (Igarashi et al., 1991). Both Gst p-2 and most theta GSTs have in common that they do not have appreciable activity with many of the substrates metabolized by other GSTs, the exception being the dog theta enzyme.

On the other hand, the OH group of the Ser10 can hydrogen bond to the carbonyl atoms of residues Arg202 and Pro203. The carbonyl atom of the latter is also hydrogen bonding to the nitrogen atom of Gly12. This would tighten the binding of the C-terminal loop.

The replacement of Arg11 by Pro in Gst p-1 results in a 97% loss of activity and an approximately 24- and 2-fold increase in the K_m for GSH and CDNB, respectively. Importantly, Stenberg et al. (1991) and Wang et al. (1993) reported a similar result when they replaced Arg12 (the equivalent to Arg11 in pi-class GSTs) in a rat (YaYa) and a human (GST2, GST B1B1) alpha-class GST with an uncharged amino acid. Arg11 is a conserved residue in pi, mu, and alpha GSTs. However, it does not directly participate in the binding of GSH and electrophilic substrates in the active site, as the marked decrease in k_{cat} and increase in the K_m value for GSH suggests. The charge of this amino acid appears important for maintaining the correct conformation of the active site. Arg11, present in the N-terminal domain, holds the helix αI in the C-terminal domain close with two hydrogen bonds (11NH2-O198 and 11Nϵ-O201) and the C-terminal tail by another two (11N-O202 and 12N-O203). Furthermore, the carbonyl oxygen of Arg11 is hydrogen bonding the amide nitrogens of Cys14 and Glu15. Arg11 therefore stabilizes the segment between strand β1 and helix αA and its position at the bottom of the active site with respect to the inner wall and the 3_{10}A helix 11−14. Arg11 has ϕ −74 and ψ −61, angles which on substitution by Pro with its fixed ϕ angle of −60 can be accommodated surprisingly well, when the C-terminal area 200−204 is moved away slightly. However, three out of the six hydrogen bonds are now lost, leading to weakened interaction with the inner wall, with the possibility of some compensation from hydrogen bonding of the hydroxyl group of Ser10 with the carbonyl atoms of 202 and 203.

The enzymes Gst p-2, P1-R11P, and P1-V10S-R11P, which contain a Pro instead of an Arg at position 11, were noticed to bind with significantly lower affinity to the GSH−agarose affinity column. This observation is consistent with the high K_m these two mutants have for GSH. The only residue close to residues 10−11 implicated in stabilizing the GSH is Arg13, which is near the terminal carboxyl group of the γ-glutamyl group of GSH. This suggests that there is a greater disturbance of the conformation than suggested by the simple model, in which no residues beyond Arg11 are affected. Residue Ser10 in Gst p-2 is positioned between two relatively rigid prolines, and the γ-turn 9−11 may not actually be present. It also cannot be excluded that the Pro has a cis conformation. Electrostatic calculations by Karshikoff et al. (1993) suggest that the Tyr 7 OH group is deprotonated by the influence of the protein charge constellation and the peptide dipoles, especially residues Gly12, Arg13, and Cys14. A drastic difference in the conformation of the 3_{10} helix 11−14 or a shift of residue Tyr 7 would have an influence on the catalytic activation.

The simultaneous replacement of Ser10 by Val and Pro11 by Arg in Gst p-2 (P2-S10V-P11R) results in an approximately 100-fold increase of k_{cat}. In contrast, an approximately 80-fold decrease in the k_{cat} of Gst p-1 is observed when Val10 and Arg11 are replaced by Ser and Pro (P1-V10S-R11P). These results provide strong evidence that the two N-terminal amino acid differences (Val/Ser, Arg/Pro) between Gst p-1 and Gst p-2 have a profound effect on the catalytic activities of these enzymes. In a recent paper by Xu and Stambrook (1994), evidence was also presented that residues 10 and 11 play an important role in determining the catalytic differences between these proteins. With both mutations present, there may be realignment of the bottom and inner wall of the active site, because of the shift of hydrogen bonding from helix αI toward the C-terminus, with possible effect on the positions of residues 202 and 205, which are close to the substrate. This might have an effect on dissociation when the GSH conjugate leaves the active site.

The single substitution of Met89 by Val has very little effect on the catalytic activity of Gst p-1. This is not surprising as this change is of a conservative nature. In addition, with the exception of mouse Gst p-1, all mammalian pi-class GSTs isolated so far have a Val residue present at position 89 (Figure 3). In the case of the *C. elegans* enzyme, this residue is conservatively replaced by Ile. Val89 in the structure of pig pi and Met89 in mouse Gst p-1 are virtually inaccessible to solvent. Although Met is slightly larger than Val, a comparison of both P1 structures does not indicate a difference in core packing. This difference, although situated in helix αD, is some distance from the active site and is therefore not expected to have a large effect on substrate binding on its own. This explains that a change from a Met to a Val in Gst p-1 leads to similar kinetic parameters.

The differences between mouse Gst p-1 and Gst p-2 do not include any of the residues involved in the contact areas within the GST dimer; therefore, Gst p-2 is expected to be a dimer. However, Val89 in mouse Gst p-2 is situated next to some residues involved in the dimer interface, Ala87, Leu88 (only marginally), Asp90, and Met91. Comparison of the mouse liver Gst p-1 and pig lung GST P1 structures does not indicate any significant differences in the dimer interface around residue 89. The only residue implicated in intersubunit stabilization of bound GSH, Asp98, is not affected.

Residues 104, 106, and 109 are in the C-terminal part of helix αD, close to residue Tyr108 which lines the H-site. The single substitution of Leu106 by Met in Gst p-1 has

very little effect on the catalytic activity. This is not surprising as the change is of a conservative nature. As for position 106, the only other pi-class GST which has a Met instead of a Leu present is the *C. elegans* enzyme. The replacement of Leu106 by a Met requires only small rearrangements to allow positioning with correct van der Waals distances in the core of the inner wall of the active site, which is unlikely to cause changes in substrate binding on its own. The nonconservative replacement of Thr109 by Arg has also little impact on the catalytic activity of Gst p-1. Thr109 is conserved in all pi-class GSTs, with the exceptions of Gst p-2 and the *C. elegans* enzyme, which both have an Arg present at this position. In the model, Arg 109 sticks out of the C-terminal part of helix αD into the large cavity between the two monomers making up the active GST dimer. It is accessible to the solvent. It is pointing away from the H-site and not directly interacting with substrates in the H-site. Because of its position it is unlikely to interfere with the substrate entering or the adduct leaving the active site. Although this difference is situated in helix αD, it is not expected to have a significant effect on substrate binding.

In contrast, the nonconservative replacement of Val104 by Gly results in an approximately 55% decrease in the k_{cat} value of Gst p-1 and a 2- and 3-fold increase in the K_m for GSH and CDNB, respectively. This finding is initially somewhat surprising, as Val104 is not conserved in the members of the pi class. Human P1-1, which has an Ile at position 104, has a similar specific activity for CDNB as mouse Gst p-1 (Mannervik & Danielson, 1988). Compared with human P1-1, the human isoform of P1-1, which has a Val at position 104, has about half the specific activity for CDNB, identical K_m for GSH, and a 4-fold increase of K_m for CDNB (Zimniak et al., 1994), data which are in very good agreement with our results. The rat pi enzyme also has a Gly present at position 104 and has much lower specific activity for CDNB than mouse Gst p-1 but not as low as mouse Gst p-2. On the basis of a comparison of human P1-1 and its Val104 isoform, Zimniak et al. (1994) have proposed that the residue at position 104 helps in defining the geometry of the H-site, with bulkier residues resulting in a smaller more restrictive H-site, while the residue may also influence activity by interacting with Tyr108 directly involved in substrate binding. Tyr108 is located within 4 Å of the Ile (or Val) at position 104 in human P1-1, suggesting that apart from size also hydrophobicity may play a role in influencing the function of 108. Since for both human P1-1 and mouse Gst p-1 the K_m for CDNB increases as the size of residue 104 decreases, a similar interpretation appears to be applicable. As in the human P1-1 structure, in the mouse Gst p-1 structure the aliphatic side chain of Val at position 104 is within van der Waals range of the ring of Tyr108, possibly keeping it in a relatively fixed position with respect to the lipophilic substrate. In mouse Gst p-2 and rat P-1 where 104 is replaced by the much smaller Gly, this stabilization will not be present at all, and the Tyr will be more free to move, which may both affect its position and ability to aid in controlling stereoselectivity, as well as its steric hindrance of dissociation of the product. CDNB may therefore be held less firmly, explaining the 3-fold increase in K_m of the mutant P1-V104G. Another possibility which needs to be considered is that because Gly can have main-chain conformations, which other residues cannot accommodate because of their size, the replacement causes a change in direction in helix αD, changing the position of Tyr108 in the active site and the size of the active site itself. In mouse Gst p-2 this might bring 108 closer to Ser10. Since no residues implicated in binding GSH are directly affected when replacing Val104 by Gly in Gst p-1, a similar K_m for GSH is expected. Ile104 in human P1-1 is at roughly van der Waals distance to the carbonyl group of the glutamic acid in GSH, possibly aiding in the catalytic reaction by stabilizing the position of the GSH in the G-site. Val in the human P1-1 isoform is at a similar distance, thus not causing a difference in K_m for GSH. In contrast, Val104 in mouse Gst p-1 is already at a distance of 6.5 Å, making such stabilization less effective. There is no possibility of such an interaction with the much smaller Gly, possibly explaining the small increase in K_m for GSH when replacing Val by Gly in Gst p-1.

The hybrid enzyme P2-S10V-P11R, which can be interpreted as a mutated Gst p-1 carrying the four mutations Met89Val, Val104Gly, Leu106Met, and Thr109Arg simultaneously, displays kinetic parameters remarkably similar to those found for the mutant P1-V104G. This finding strongly suggests that the four amino acids present in Gst p-2 at positions 89, 104, 106, and 109 do not affect the catalytic activity in a combined way.

In conclusion, primary sequence analysis, catalytic activity, and kinetic analysis clearly identify Gst p-1 as the major pi-class GST isolated from mouse liver. Gst p-2 displays very low conjugating activity of various electrophilic substrates with glutathione, very low selenium-independent peroxidase activity, and no isomerase activity toward Δ^5-androstene-3,17-dione. Three out of the six amino acid differences occurring between the two enzymes are responsible for the loss of activity of Gst p-2; these are Ser10, Pro11, and Gly104. To determine the significance of these changes will require further structural studies. Whether Gst p-2 has a specific function in relation to Gst p-1 also remains to be determined.

ACKNOWLEDGMENT

We thank Dr. L. I. McLellan and Dr. J. D. Hayes for the generous gifts of Yf marker isolated from mouse liver, a polyclonal antibody raised against murine Yf, and Δ^5-androstene-3,17-dione. We also gratefully acknowledge Dr. T. J. Mantle for his advice on kinetic analysis.

REFERENCES

Bammler, T. K., Smith, C. A. D., & Wolf, C. R. (1994) *Biochem. J. 298*, 385−390.

Batist, G., Tulpule, A., Sinha, B. K., Katki, A. G., Meyers, C. E., & Cowan, K. H. (1986) *J. Biol. Chem. 261*, 5544−5549.

Benson, A. M., Talalay, P., Keen, J. H., & Jakoby, W. B. (1977) *Proc. Natl. Acad. Sci. U.S.A. 74*, 158−162.

Black, S. M., & Wolf, C. R. (1991) *Pharmacol. Ther. 51*, 139−154.

Coles, B., & Ketterer, B. (1990) *Crit. Rev. Biochem. Mol. Biol. 25*, 47−70.

Cowan, K. H., Batist, G., Tulpule, A., Sinha, B. K., & Myers, C. E. (1986) *Proc. Natl. Acad. Sci. U.S.A. 83*, 9328−9332.

Dirr, H. W., Mann, K., Huber, R., Ladenstein, R., & Reinemer, P. (1991) *Eur. J. Biochem. 196*, 693−698.

Garcia-Saez, I., Parraga, A., Phillips, M. F., Mantle, T. J., & Coll, M. (1994) *J. Mol. Biol. 237*, 298−314.

Habig, W. H., & Jakoby, W. B. (1981) *Methods Enzymol. 77*, 398−405.

Habig, W. H., Pabst, M. T., & Jakoby, W. B. (1974) *J. Biol. Chem. 249*, 7130−7139.
Hatayama, I., Satoh, K., & Sato, K. (1990) *Nucleic Acids Res. 18*, 4606.
Hayes, J. D., & Clarkson, G. H. D. (1982) *Biochem. J. 207*, 459−470.
Hernando, N., Martin-Alonso, J. M., Ghosh, S. & Coca-Prados, M. (1991) GenBank entry X61233.
Howie, A. F., Forrester, L. M., Glancey, M. J., Schlager, J. J., Powis, G., Beckett, G. J., Hayes, J. D., & Wolf, C. R. (1990) *Carcinogenesis 11*, 451−458.
Igarashi, T., Kohara, A, Shikata, Y., Sagami, F., Sonoda, J., Hoeie, T., & Satoh, T. (1991) *J. Biol. Chem. 266*, 21709−21717.
Ivanetich, K., & Goold, K. D. (1989) *Biochim. Biophys. Acta 998*, 7−13.
Ji, X., Zhang, P., Armstrong, R. N., & Gilliland, G. L. (1992) *Biochemistry 31*, 10169−10184.
Ji, X., Johnson, W. W., Sesay, M. A., Dickert, L., Prasad, S. M., Ammon, H. L., Armstrong, R. N., & Gilliland, G. L. (1994) *Biochemistry 33*, 1043−1052.
Jones, T. A. J. (1978) *J. Appl. Crystallogr. 11*, 268−272.
Kabsch, W., & Sander, C. (1983) *Biopolymers 22*, 2577−2637.
Kano, T., Sakai, M., & Muramatsu., M. (1987) *Cancer Res. 47*, 5626−5630.
Karshikoff, A., Reinemer, P., Huber, R., & Ladenstein, R. (1993) *Eur. J. Biochem. 215*, 663−670.
Ketterer, B., Tan, K. H., Meyer, D. J., & Coles, B. (1987) in *Glutathione S-transferases and carcinogenesis* (Mantle, T. J., Pickett, C. B., & Hayes, J. D., Eds.) p 149, Taylor & Francis, London.
Laemmli, U. K. (1970) *Nature* (London) *227*, 680−685.
Listowsky, I., Abramovitz, M., Homma, H., & Niitsu, Y. (1988) *Drug Metab. Rev. 19*, 305−318.
Lowry, O. H., Rosebrough, N. J., Farr, A. L., & Randall, R. J. (1951) *J. Biol. Chem. 193*, 265−275.
Mannervik, B., & Danielson U. H. (1988) *CRC Crit. Rev. Biochem. 23*, 283−337.
Mannervik, B., Alin, P., Guthenberg, C., Jensson, H., Tahir, M. K., Warholm, M., & Jornvall, H. (1985) *Proc. Natl. Acad. Sci. U.S.A. 82*, 7202−7206.
Mannervik, B., Awasthi, Y. C., Board, P. G., Hayes, J. D., Di Ilio, C., Ketterer, B., Listowsky, I., Morgenstern, R., Muramatsu, M., Pearson, W. R., Pickett, C. B., Sato, K., Widersten, M., & Wolf, C. R. (1992) *Biochem. J. 282*, 305.
McLellan, L. I., & Hayes, J. D. (1987) *Biochem. J. 245*, 399−406.
Meyer, D. J., Coles, B., Pemble, S. E., Gilmore, K. S., Fraser, G. M., & Ketterer, B. (1991) *Biochem. J. 274*, 409−414.
Phillips, M. F., & Mantle, T. J. (1991) *Biochem. J. 275*, 703−709.
Reddy, C. C., Tu, C-P. D., Burgess, J. R., Ho, C. Y., Scholz, R. W., & Massaro, E. J. (1981) *Biochem. Biophys. Res. Commun. 101*, 970−978.
Reinemer, P., Dirr, H. W., Ladenstein, R., Schaeffer, J., Gallay, O., & Huber, R. (1991) *EMBO J. 10*, 1997−2005.
Reinemer, P., Dirr, H. W., Ladenstein, R., Huber, R., LoBello, M. L., Federici, G., & Parker, M. W. (1992) *J. Mol. Biol. 227*, 214−226.
Sanger, F., Nicklen, S., & Coulson, A. R. (1977) *Proc. Natl. Acad. Sci. U.S.A. 74*, 5463−5467.
Sato, K. (1989) *Adv. Cancer Res. 52*, 205−255.
Sato, K., Kitahara, A., Satoh, K., Ishikawa, T., Tatematsu, M., & Ito, N. (1984a) *Gann 75*, 199−202.
Sato, K., Satoh, K., Kitahara, A., Ishikawa, T., Soma, Y., Tatematsu, M., & Ito, N. (1984b) *Proc. Am. Assoc. Cancer Res. 25*, 7.
Sinning, I., Kleywegt, G. J., Cowan, S. W., Reinemer, P., Dirr, H. W., Huber, R., Gilliland, G. L., Armstrong, R. N., Ji, X., Board, P. G., Olin, B., Mannervik, B. & Jones, T. A. (1993) *J. Mol. Biol. 232*, 192−212.
Stenberg, G., Board, P. G., Carlberg, I., & Mannervik, B. (1991) *Biochem. J. 274*, 549−555.
Suguoka, Y., Kano, T., Okuda, A., Sakai, M., Kitagawa, T., & Muramatsu, M. (1985) *Nucleic Acids Res. 13*, 6049−6057.
Swedmark, S., & Jensson, D. (1994) *Gene 139*, 251−256.
Volm, M., Mattern, J., & Samsel, B. (1991) *Br. J. Cancer 64*, 700−704.
Wang, R. W., Newton, D. J., Johnson, A. R., Pickett, C. B., & Lu, A. Y. H (1993) *J. Biol. Chem. 268*, 23981−23985.
Warholm, M., Jensson, H., Tahir, M. K., & Mannervik, B. (1986) *Biochemistry 25*, 4119−4125.
Weston, K., Yochem, J., & Greenwald, I. (1989) *Nucleic Acids Res. 17*, 2138.
Wolf, C. R., Wareing, C. J., Black, S. M., & Hayes, J. D. (1990) Glutathione S-transferases in Resistance to Chemotherapeutic Drugs, in *Glutathione S-transferases and Drug Resistance* (Hayes, J. D., Pickett, C. B., & Mantle, T. J., Eds.) pp 296−307, Taylor and Francis, London.
Xu, X., & Stambrook, P. J. (1994) *J. Biol. Chem. 269*, 30268−30273.
Zimniak, P., Nanduri, B., Pikula, S., Bandorowicz-Pikula, J., Singhal, S. S., Srivastava, S. K., Awasthi, S., & Awasthi, Y. C. (1994) *Eur. J. Biochem. 224*, 893−899.

BI950244+